A Novel Target-Field Approach to Design Bi-Planar Shim Coils for Permanent-Magnet MRI

WENTAO LIU, XIN TANG, DONGLIN ZU

Institute of Heavy Ion Physics, Beijing Key Laboratory of Medical Physics and Engineering, Physics school, Peking University, Beijing 100871, China

ABSTRACT: A novel target-field approach for designing bi-planar gradient and shim coils of restricted radius for use with permanent-magnet MRI systems is presented in this article. The method is based on identification of the weighting of harmonic components in the current distribution that will generate a magnetic field whose *z*-component follows a chosen spherical harmonic function. Mathematical expressions that relate the harmonic terms in the surface current distribution to spherical harmonic terms in the field expansion are established and then used in a simple matrix inversion approach to design a range of shim coils. The expressions providing a spherical harmonic decomposition of the field components produced by a particular current distribution are novel. The results can be used to design bi-planar shim coils of restricted radius that will generate a field variation that follows a certain spherical harmonic over a reasonably-sized volume. A stream function was utilized to obtain the discrete wire distribution on the coil plane. This method does not require the setting of the target-field points. Through an analysis of the matrix equations in terms of condition numbers, we show that this novel approach has no ill-conditioned problems. © 2010 Wiley Periodicals, Inc. Concepts Magn Reson Part B (Magn Reson Engineering) 37B: 29–38, 2010

KEY WORDS: active shimming; bi-planar shim coil; permanent-magnet MRI; target-field approach; spherical harmonics

INTRODUCTION

Romeo and Hoult (*1*) presented a full mathematical framework for designing shim coils on a cylindrical-surface for MRI systems with solenoidal superconducting magnets. They used spherical harmonics to series expand the magnetic field over a target-diameter-sphere-volume (DSV) of interest (*2*, *3*). To improve the field homogeneity over the DSV, each shim coil, responsible for adjusting one such harmonic, needs to be tuned to annul the zonal or tesseral harmonic fields. By combining current elements from various shapes, such as loop arcs, ellipse arcs, etc., one can enhance the harmonic of interest and eliminate unnecessary harmonics. Unfortunately, the qualified volume calculated from this method is less than the desired specification; thus, such a classical method has limitations for advanced shim coil design.

An alternative method to obtain considerably larger usable volumes is the "target field" method proposed by Turner (*4*, *5*). This method has no ill-conditioned problem because Fourier transforms have unique inverses. In the original target-field approach (*4*), there is no explicit constraint on coil length, which may result in unnecessarily long

Received 11 June 2009; revised 30 November 2009; accepted 4 December 2009

Correspondence to: Donglin Zu; E-mail: dlzu@pku.edu.cn

Concepts in Magnetic Resonance Part B (Magnetic Resonance Engineering), Vol. 37B(1) 29–38 (2010)

Published online in Wiley InterScience (www.interscience.wiley.com). DOI 10.1002/cmr.b.20153

coils. Therefore, to restrict the coil length, Turner (*5*) improved this method by adding a constraint that the surface current must fall to zero outside of a finite interval. As a compromise, however, it degrades the target-field method as discussed by Jin (*6*).

For permanent-magnet MRI systems, the spatial homogeneity over the region of interest (0.3 m DSV in this article) needs to be controlled at the order of 10^{-5} or smaller relative to the main magnetic field strength B_0. Brideson et al. (*7*) utilized target-field and Fourier Integral methods to design bi-planar shim and gradient coils for C-type permanent magnets. Liu and Truwit attempted the design of bi-planar coils of restricted radius (*8*). As soon as the coil size is restricted, however, the target-field approach leads to a Fredholm integral equation; as a result, an ill condition exists with it. To overcome the ill condition with the integral equation, Forbes and Crozier used a minimization technique combined with Tikhonov regularization to solve the surface current on the coil plane (*9*, *10*). The linear programming algorithm for shim design (*11*) embodies much flexibility for MRI systems of complex geometry. Liu et al. (*12*) overcame the ill-conditioned problems for gradient-coil design by selecting a collection of the target-field points properly instead of using Tikhonov regularization. However, this method seems invalid for designing higher-order shim coils (see "Discussion" section). In this article, we combine the classical harmonics approach (*1*, *3*) and the target-field approach (*4*, *5*, *9*, *10*, *12*) to design bi-planar shim coils with finite radius. To our knowledge, this is the first time that the relationship between a set of surface current coefficients (corresponding to each order and each degree harmonic) and the harmonic field coefficient itself has been established.

THEORY

Figure 1 shows the geometry of bi-planar shim coils and the spherical polar coordinate systems used here. The shim coils are located at a pair of planes $z = \pm a$, respectively, and the maximum radii are ρ_a; $\vec{r}(r, \theta, \phi)$ is the field point in the imaging volume and $\vec{r}'(f, \alpha, \psi)$ is one source point on the coil planes. The shim coil may be idealized to be on two parallel planes on which a surface current $\vec{J}(\rho, \psi)$ is flowing. The surface current in polar coordinates system is expressed as $\vec{J} = J_\psi \hat{e}_\psi + J_\rho \hat{e}_\rho$. The vector $\hat{e}_\psi$ denotes the unit vector in the ψ-direction, with a similar notation applying for the other unit basis

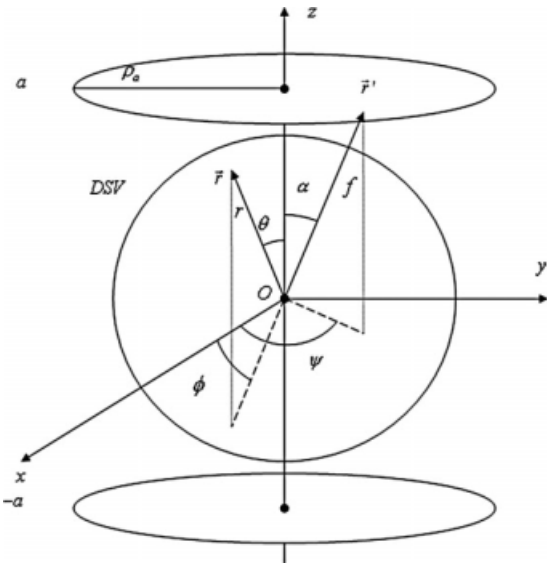

Figure 1 Schematic diagram showing the spherical polar coordinate systems for describing the bi-planar current and the field it produces.

vectors. The components J_ρ and J_ψ satisfy the steady-state continuity equation $\frac{\partial}{\partial \rho}(\rho J_\rho) + \frac{\partial J_\psi}{\partial \psi} = 0$. It follows at once from the continuity equation that the two components of the surface current on the coil planes can be expressed in terms of a single stream function $S(\rho, \psi)$ according to the relations

$$J_\rho = \frac{\partial S}{\rho \partial \psi}, \quad J_\psi = -\frac{\partial S}{\partial \rho}. \qquad [1]$$

For the bi-planar shim coils, $z = \pm a = f \cos\alpha$, and $\rho = f \sin\alpha$ (see Fig. 1). The stream function can be set as:

$$S^{\pm}(\rho, \psi) = (\pm 1)^{l+k} \cos k\psi \sum_{q=1}^{Q} U_q s_q(\rho),\ 0 \le \rho \le \rho_a \qquad [2]$$

where l and k are two nonnegative integer parameters (*1*) of the coils that we call the "order" and "degree" of the coils, respectively. However, in the following analyses, we will find that they are related to the order and degree of the harmonic fields generated by the coils. The sign "$\pm$" denotes the top and bottom plane, respectively, and the basis functions $s_q(\rho)$ can be set arbitrarily as the simple trigonometric function $s_q(\rho) = \sin\frac{q\pi\rho}{\rho_a}$. The components of the surface current can be written as

$$\begin{cases} J_{\psi}^{\pm} = (\pm 1)^{l+k} \cos k\psi \sum_{q=1}^{Q} U_q j_{\psi,q}(\rho) \\ J_{\rho}^{\pm} = (\pm 1)^{l+k} \sin k\psi \sum_{q=1}^{Q} U_q j_{\rho,q}(\rho) \end{cases}. \quad [3]$$

where $j_{\psi,q}(\rho)$, $j_{\rho,q}(\rho)$ satisfy:

$$j_{\psi,q}(\rho) = -\frac{\partial s_q(\rho)}{\partial \rho}, \quad j_{\rho,q}(\rho) = -\frac{k}{\rho} s_q(\rho). \quad [4]$$

U_qs in Eq. [3] are the Fourier coefficients for the unknown surface current, and the number of terms Q in the series expansion of the current should be chosen large enough to satisfy the required accuracy. In general, the surface currents on the top and bottom planes have the same distribution but not necessarily the same direction of flow. When $l + k$ is even (odd), the magnetic field B_z has even (odd) symmetry with respect to the $z = 0$ plane and the current directions on the pair of planes of the coil are the same (opposite).

Now turning to the magnetic field that the surface current generates, following the analysis of Romeo and Hoult (*1*) over a spherical region with radius $r < f_{\min} = a$, the Green's function $\frac{1}{|\vec{r}-\vec{r}'|}$ can be expressed as

$$\frac{1}{|\vec{r}-\vec{r}'|} = \frac{1}{f} \sum_{n=0}^{\infty} \sum_{m=0}^{n} \varepsilon_m \frac{(n-m)!}{(n+m)!} P_{nm}(\cos\alpha) \left(\frac{r}{f}\right)^n \times P_{nm}(\cos\theta) \cos[m(\phi - \psi)], \; \varepsilon_m = \begin{cases} 1 & m = 0 \\ 2 & m \neq 0 \end{cases}, \quad [5]$$

where $P_{nm}(x)$ is associated Legendre function. If $m = 0$, i.e., $P_{n0} = P_n$, ($n = 1, 2, \ldots$), they are the Legendre functions that possess cylindrical symmetry. According to the Biot-Savart law (*13*) and considering $\frac{\vec{r}-\vec{r}'}{|\vec{r}-\vec{r}'|^3} = -\nabla \frac{1}{|\vec{r}-\vec{r}'|}$, the magnetic field generated by the surface current is

$$d\vec{B} = \frac{\mu_0}{4\pi} \nabla \frac{1}{|\vec{r}-\vec{r}'|} \times \vec{J}\, d\sigma', \quad [6]$$

where the constant μ_0 is the magnetic permeability of free space, and $d\sigma' = \rho d\rho d\psi$. As is usual for MRI applications, we consider only the z component of $d\vec{B}$. If we let $\vec{A} = \nabla \frac{1}{|\vec{r}-\vec{r}'|}$, because $\nabla\Phi = \frac{\partial\Phi}{\partial r}\hat{e}_r + \frac{1}{r}\frac{\partial\Phi}{\partial\theta}\hat{e}_\theta + \frac{1}{r\sin\theta}\frac{\partial\Phi}{\partial\phi}\hat{e}_\phi$, and $\nabla \frac{1}{|\vec{r}-\vec{r}'|} = -\nabla' \frac{1}{|\vec{r}-\vec{r}'|}$, the z component of $d\vec{B}$ is

$$\begin{aligned} dB_z &= \frac{\mu_0}{4\pi} d\sigma' (A_x J_y - A_y J_x) \\ &= \frac{\mu_0}{4\pi} d\sigma' [(A_f \sin\alpha\cos\psi + A_\alpha \cos\alpha\cos\psi \\ &\quad - A_\psi \sin\psi)(J_\psi \cos\psi + J_\rho \sin\psi) \\ &\quad - (A_f \sin\alpha \sin\psi + A_\alpha \cos\alpha \sin\psi + A_\psi \cos\psi) \\ &\quad \times (-J_\psi \sin\psi + J_\rho \cos\psi)] \\ &= \frac{\mu_0}{4\pi} d\sigma' (A_f J_\psi \sin\alpha + A_\alpha J_\psi \cos\alpha - A_\psi J_\rho) \\ &= \frac{\mu_0}{4\pi} d\sigma' \sum_{n=0}^{\infty} \sum_{m=0}^{n} \varepsilon_m \frac{(n-m)!}{(n+m)!} \frac{r^n}{f^{n+2}} \\ &\quad \times P_{nm}(\cos\theta)[(n+1) J_\psi \sin\alpha P_{nm}(\cos\alpha) \\ &\quad \times \cos m(\phi - \psi) - J_\psi \cos\alpha \frac{\partial P_{nm}(\cos\alpha)}{\partial\alpha} \\ &\quad \times \cos m(\phi - \psi) + m J_\rho \frac{P_{nm}(\cos\alpha)}{\sin\alpha} \\ &\quad \times \sin m(\phi - \psi)]. \end{aligned} \quad [7]$$

Differentiation of Ferrer's-associated Legendre polynomials is described on page 334 of (*14*):

$$\frac{dP_{nm}(\cos\alpha)}{d\alpha} = \frac{1}{\sin\alpha}[(n-m+1) P_{n+1,m}(\cos\alpha) - (n+1)\cos\alpha\, P_{nm}(\cos\alpha)]. \quad [8]$$

By Inserting Eq. [8] into [7], implementing some algebra operations, and letting

$$\begin{cases} \frac{(n-m)!}{(n+m)!} \frac{1}{f^{n+2}} = C_{nm}; \; m \frac{P_{nm}(\cos\alpha)}{\sin\alpha} = C_{nm}^{\rho} \\ \frac{1}{\sin\alpha}[(n+1) P_{nm}(\cos\alpha) - (n-m+1)\cos\alpha\, P_{n+1,m}(\cos\alpha)] = C_{nm}^{\psi} \end{cases} \quad [9]$$

we recast Eq. [7] as

$$\begin{aligned} dB_z &= \frac{\mu_0}{4\pi} d\sigma' \sum_{n=0}^{\infty}\sum_{m=0}^{n} \varepsilon_m C_{nm} r^n P_{nm}(\cos\theta) \\ &\quad \times [C^{\psi}_{nm} J_\psi \cos m(\phi-\psi) + C^{\rho}_{nm} J_\rho \sin m(\phi-\psi)] \\ &= \frac{\mu_0}{4\pi} d\sigma' \sum_{n=0}^{\infty}\sum_{m=0}^{n} \varepsilon_{\mathrm{m}} C_{nm} r^n P_{nm}(\cos\theta) \\ &\quad \times [\cos m\phi (C^{\psi}_{nm} J_\psi \cos m\psi - C^{\rho}_{nm} J_\rho \sin m\psi) \\ &\quad + \sin m\phi (C^{\psi}_{nm} J_\psi \sin m\psi + C^{\rho}_{nm} J_\rho \cos m\psi)] \end{aligned} \quad [10]$$

By surveying carefully the content in square brackets in Eq. [10], one sees that they have the form of a scalar product of two vectors. Hence, we can introduce a two-dimensional row vector:

$$D'_{nm} = \frac{\mu_0}{4\pi} d\sigma' \varepsilon_m C_{nm} (C^{\psi}_{nm} J_\psi \cos m\psi - C^{\rho}_{nm} J_\rho \sin m\psi, \quad C^{\psi}_{nm} J_\psi \sin m\psi + C^{\rho}_{nm} J_\rho \cos m\psi); \quad [11]$$

thus, Eq. [10] can be simplified as

$$dB_z = \sum_{n=0}^{\infty}\sum_{m=0}^{n} D'_{nm} r^n P_{nm}(\cos\theta) \begin{pmatrix} \cos m\phi \\ \sin m\phi \end{pmatrix}. \quad [12]$$

We should point out that the bi-planar surface currents J_ψ, J_ρ in Eq. [11] include $J^{\pm}_{\psi}, J^{\pm}_{\rho}$, respectively. Substituting the expression (11) into Eq. [12] and integrating it, gives

$$B_z = \sum_{n=0}^{\infty}\sum_{m=0}^{n} D_{nm} r^n P_{nm}(\cos\theta) \begin{pmatrix} \cos m\phi \\ \sin m\phi \end{pmatrix}. \quad [13]$$

Here the harmonic coefficients are

$$D_{nm} = \frac{\mu_0}{4\pi} \int_0^{\rho_a}\int_0^{2\pi} \rho\, d\psi\, d\rho\, \varepsilon_m C_{nm} \begin{pmatrix} \left(C^{\psi+}_{nm} J^{+}_{\psi} + C^{\psi-}_{nm} J^{-}_{\psi}\right)\cos m\psi - \left(C^{\rho+}_{nm,} J^{+}_{\rho} + C^{\rho-}_{nm} J^{-}_{\rho}\right)\sin m\psi \\ \left(C^{\psi+}_{nm} J^{+}_{\psi} + C^{\psi-}_{nm} J^{-}_{\psi}\right)\sin m\psi + \left(C^{\rho+}_{nm} J^{+}_{\rho} + C^{\rho-}_{nm} J^{-}_{\rho}\right)\cos m\psi \end{pmatrix}^T,$$

where the superscript T denotes transpose. Substituting Eq. [3] into the above equation, we obtain

$$\begin{aligned} D_{nm} = \frac{\mu_0}{4\pi} \sum_{q=1}^{Q} U_q \int_0^{\rho_a}\int_0^{2\pi} \rho\, d\psi\, d\rho\, \varepsilon_m C_{nm} \\ \times \begin{pmatrix} \left[C^{\psi+}_{nm} + (-1)^{l+k} C^{\psi-}_{nm}\right] j_{\psi,q} \cos k\psi \cos m\psi - \left[C^{\rho+}_{nm} + (-1)^{l+k} C^{\rho-}_{nm}\right] j_{\rho,q} \sin k\psi \sin m\psi \\ \left[C^{\psi+}_{nm} + (-1)^{l+k} C^{\psi-}_{nm}\right] j_{\psi,q} \cos k\psi \sin m\psi + \left[C^{\rho+}_{nm} + (-1)^{l+k} C^{\rho-}_{nm}\right] j_{\rho,q} \sin k\psi \cos m\psi \end{pmatrix}^T. \end{aligned} \quad [14]$$

According to the parity of associated Legendre function: $P_{nm}(-\cos\alpha) = (-1)^{n+m} P_{nm}(\cos\alpha)$ [refer to page 333 of (*14*)], and the orthogonality of trigonometric functions:

$$\begin{cases} \int_0^{2\pi} \sin k\psi \sin m\psi\, d\psi = (\varepsilon_m - 1)\pi\delta_{km} \\ \int_0^{2\pi} \cos k\psi \cos m\psi\, d\psi = 2\pi\delta_{km}/\varepsilon_m \\ \int_0^{2\pi} \sin k\psi \cos m\psi\, d\psi = 0, \end{cases} \quad [15]$$

Equation (13) is reduced to

$$\begin{aligned} D_{nm} = \frac{\mu_0}{2} \int_0^{\rho_a} \rho\, d\rho\, C_{nm} \sum_{q=1}^{Q} U_q \\ \times \begin{pmatrix} \left[1 + (-1)^{n+m+l+k}\right] \delta_{k,m} \left(C^{\psi}_{nm} j_{\psi,q} - C^{\rho}_{nm} j_{\rho,q}\right) \\ 0 \end{pmatrix}. \end{aligned} \quad [16]$$

For an l-th order and k-th degree shim coil, only a special order and degree of harmonic magnetic field,

$$T_{nm} = r^n P_{nm}(\cos\theta)\cos m\phi, \quad [17]$$

can be generated. In Eq. [17] the m and n satisfy

$$\begin{cases} m = k \\ n = k + (l+k) \bmod 2 + 2(i-1), (i = 1, 2, \cdots). \end{cases} \quad [18]$$

It is assumed here that the harmonic fields exhibit either even or odd symmetry with respect to the $z = 0$ plane. This is justified by the fact that the fields will be chosen to have forms given by spherical harmonics. Thus, the coefficients in Eq. [16] are simplified as

$$D(i) = \mu_0 \int_0^{\rho_a} \rho \, d\rho \, C_{nk} \sum_{q=1}^{Q} U_q \left(C_{nk}^{\psi} j_{\psi,q} - C_{nk}^{\rho} j_{\rho,q} \right), \quad [19]$$

Picking up the current coefficients U_q and applying Eq. [4], we can obtain a coefficient matrix whose elements are

$$D(i,q) = \mu_0 \int_0^{\rho_a} \rho \, d\rho \, C_{nk} \left(C_{nk}^{\rho} \frac{k}{\rho} s_q(\rho) - C_{nk}^{\psi} \frac{\partial s_q(\rho)}{\partial \rho} \right). \quad [20]$$

Consequently, for the coil of the l-th order and k-th degree, the final magnetic field is expanded as

$$B_z = \sum_{n=1}^{\infty} \sum_{q=1}^{Q} U_q D(i,q) r^n P_{nk}(\cos\theta) \cos k\phi. \quad [21]$$

To find the Fourier coefficients $U = \left(U_1, U_2, \cdots, U_Q\right)^T$ of the unknown surface current, we set a column vector of target harmonic coefficients,

$$A = \begin{pmatrix} A_1 & A_2 & \cdots & A_N \end{pmatrix}^T. \quad [22]$$

Here the integer N satisfies the condition $Q \geq N \geq (l-k)/2 + 1$, and the i-th element is

$$A_i = \delta_{l,n} b_{nm} = \delta_{l,k+(l+k)\mathrm{mod}2+2(i-1)} b_{nm}, \quad [23]$$

where b_{nm} is the target harmonic coefficient of the n-th order and m-th degree. When $n = 1$ this defines a linear gradient suitable for both encoding and shimming; when $n \geq 2$ this defines a higher-order coefficient useful for shimming only. Finally, we obtain a matrix equation

$$DU = A; \quad [24]$$

thus, U can be obtained as

$$U = D^{-1}A. \quad [25]$$

As a result, the Fourier coefficients of the unknown surface current for an assigned harmonic can be found. Once the coefficients U_q are found, the stream functions on the coil planes can be calculated from Eq. [2]. The surface current as well as the coil winding patterns on the coil planes are now immediately available from Eq. [1], simply in the form of contours, drawn as the stream function with equally spaced intervals (*15*).

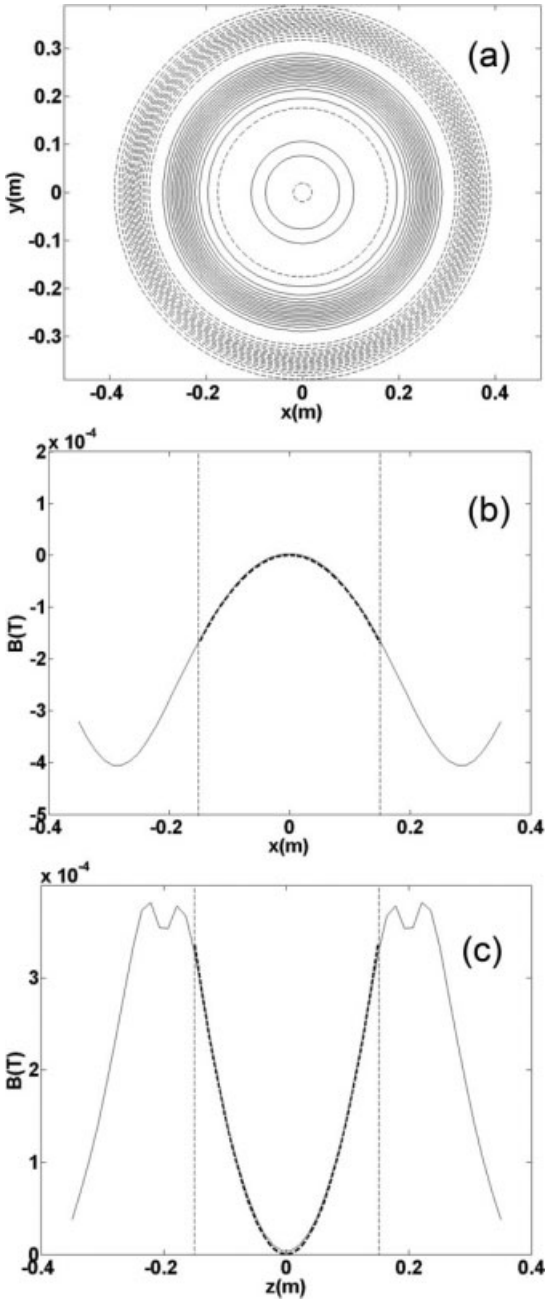

Figure 2 The winding pattern of the *T*20 shim coil (a), and the magnetic field it generates along the *x*-axis (b) and *z*-axis (c).

METHODS

Numerical simulation was carried out in Matlab (The Mathworks, Natick, MD). The spherical harmonics

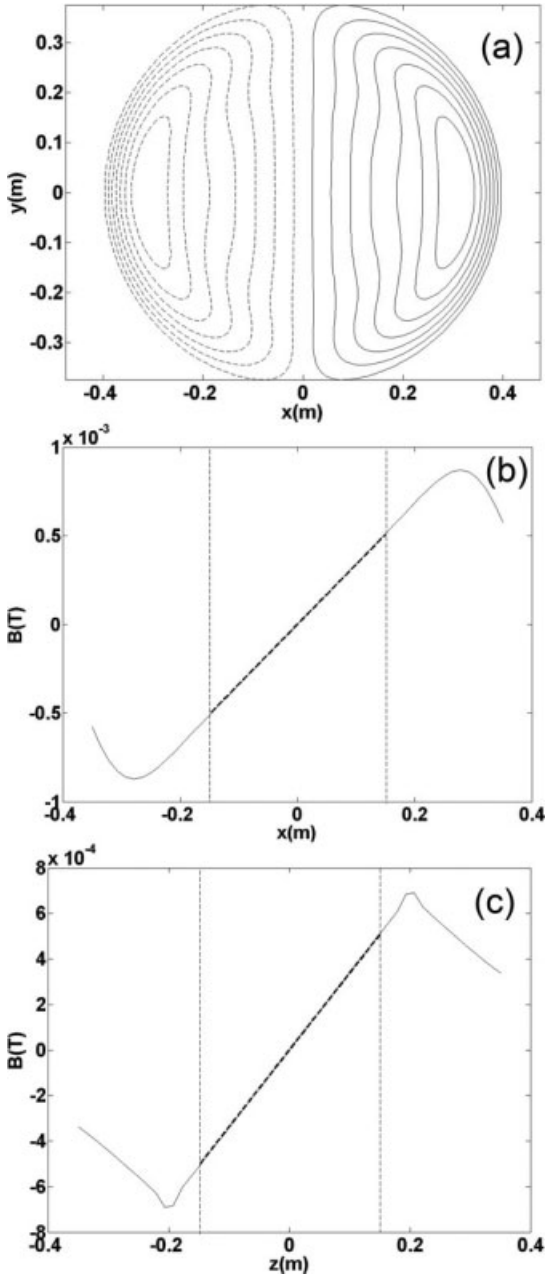

Figure 3 The winding pattern of the *T*21 shim coil (a), and the magnetic field it generates along the *x*-axis (b) and *z*-axis (c).

were divided into two subsets: zonal ($m = 0$) and tesseral ($m \neq 0$) harmonics. To illustrate how to set a target harmonic field coefficient vector A, we will discuss a few typical cases as follows.

Case 1

For a linear z-gradient coil with target gradient strength G_z, the target field is written as $B_z = G_z r P_{10}(\cos\theta)$, with $n = 1$ and $m = 0$. Thus, the order of the z-gradient coil should be set as $l = 1$ and the degree $k = 0$. From Eq. [18], $n = 1 + 2(i-1), i = 1, 2, 3, \cdots$. This type of coil includes not only zonal harmonic T_{10}, but also T_{30}, T_{50},..., in which the harmonic coefficients are A_1,A_2,A_3,..., respectively. Therefore, to design a T_{10} shim coil with target coefficient G_z, we should set $A_1 = G_z$ and the other harmonic coefficients as $A_2 = A_3 = \cdots A_N = 0$. In summary, the target harmonic field coefficient vector should be set as

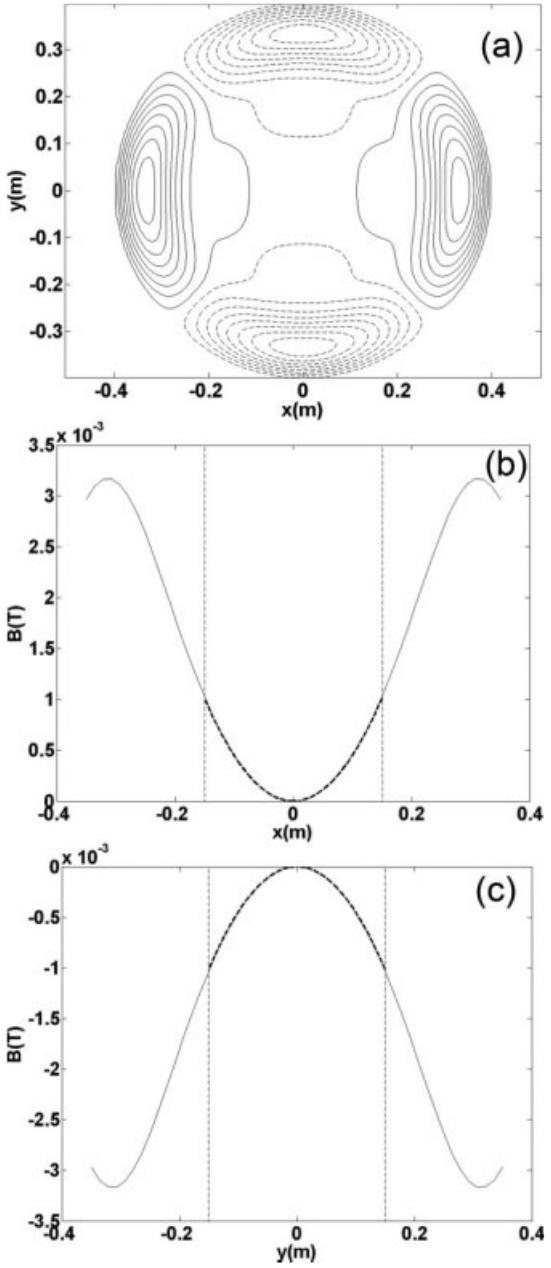

Figure 4 The winding pattern of the *T*22 shim coil (a), and the magnetic field it generates along the *x*-axis (b) and *z*-axis (c).

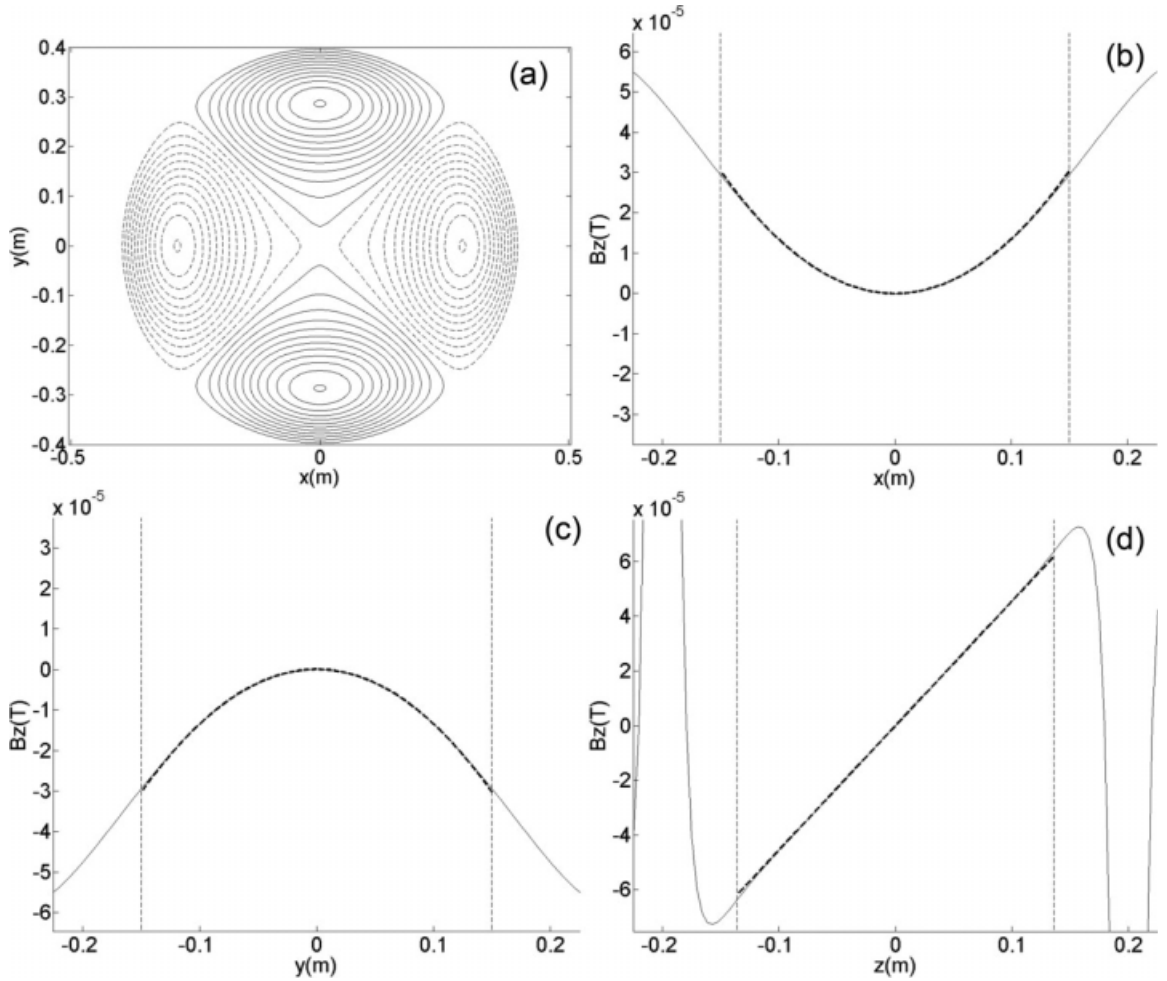

Figure 5 The winding pattern of the $T32$ shim coil (a), and the magnetic field it generates along the x-axis (b), y-axis (c), and z-axis (d).

$A = (G_z\ 0\ \ldots\ 0)^T$, where we use G_z to indicate the linear z-gradient strength b_{10}.

Case 2

For a quadratic order zonal harmonic field $(B_z)_{20} = b_{20}r^2\,P_{20}(\cos\theta)$ with $n = 2$ and $m = 0$, the order of the harmonic coil should be set as $l = 2$ and the degree $k = 0$. As required by Eq. [18], $n = 0,2,4,\cdots$. This type of coil can generate zonal harmonics of T_{00}, T_{20}, T_{40},..., in which the harmonic coefficients are A_1, A_2, A_3,..., respectively. Correspondingly we set the target harmonic field coefficient vector as $A = (0\ b_{20}\ 0\ \cdots\ 0)^T$.

Case 3

For cubic order tesseral harmonic field $(B_z)_{32} = b_{32}r^3\,P_{32}(\cos\theta)\cos 2\phi$ with $n = 3$ and $m = 2$. The order of the shim coils should be set as $l = 3$ and the degree $k = 2$. Based on Eq. [18], $n = 3 + 2(i-1), i = 1,2,3,\cdots$ we can set $n = 3,5,7,\cdots$. This type of coil can generate harmonics T_{32},T_{52},T_{72},.... To design T_{32} shim coil, we should set the target harmonic field coefficient vector as $A = (b_{32}\quad 0\quad 0\quad \cdots\quad 0)^T$.

Over all, any pure zonal shim coil and one-half of all possible tesseral shim coils can be directly designed using this novel method. The other half of tesseral shim coils can be obtained by rotating their counterparts with a proper angle (to be discussed later). Therefore, as long as the geometry parameters for the bi-planar shim coil corresponding to the n^{th} order the k^{th} degree harmonic b_{nk} are given, we can compute the surface current coefficients U_q of the l^{th} order the k^{th} degree harmonic coil through Eq. [25]. Once the coefficients U_q have been determined, the stream function $S^{\pm}(\rho,\psi)$ in Eq. [2] will be determined. Finally, the

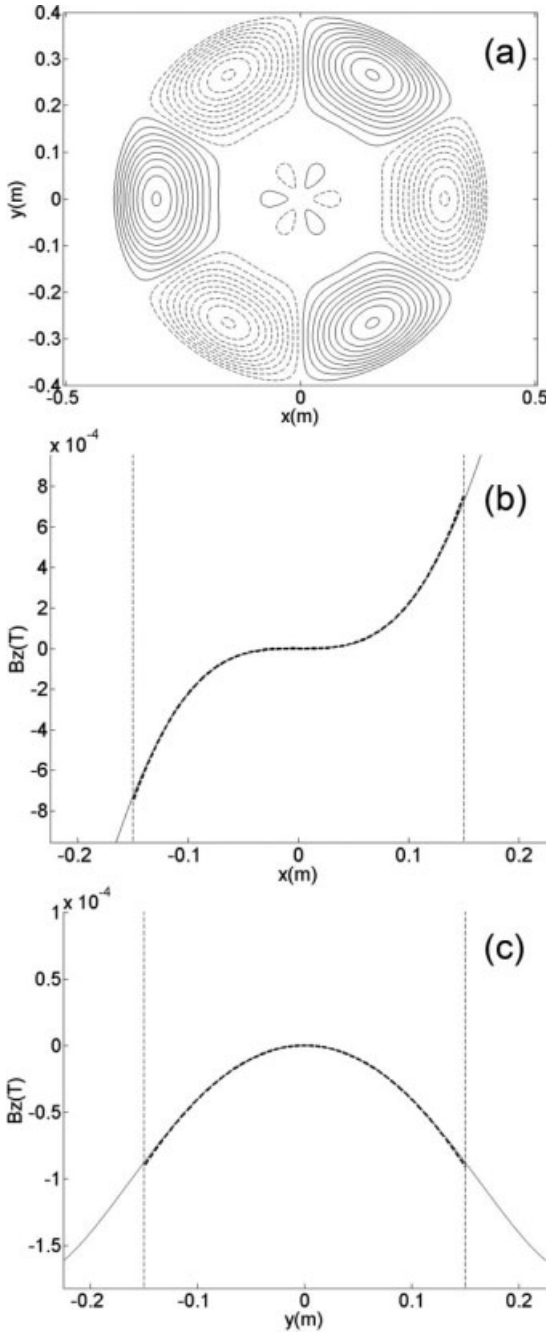

Figure 6 The winding pattern of the $T33$ shim coil (a), and the magnetic field it generates along the x-axis (b) and y-axis (c).

winding patterns of the coils can be directly obtained by contouring the stream function.

RESULTS

Figures 2(a)–6(a) show the coil winding patterns obtained with this novel method for the harmonics T_{20}, T_{21}, T_{22}, T_{32}, and T_{33}, respectively. In these examples, the coils are located at $z = \pm a$, $a = 0.2$ m, and their maximum radius is $\rho_a = 0.40$ m. The target field is located over a 0.3 m DSV. In all figures, the dashed versus solid lines in the winding patterns indicate counter-flowing currents. The B_z-field produced by these coils, as a function of (x, z), (x, y), or (x, y, z), are shown in (b) and (c) or (b), (c) and (d) of Fig. 2–6, respectively. These spherical harmonics are evaluated at the target region over a 0.3 m DSV. The fields generated by the discrete currents (thin solid curves) show mostly excellent agreement with the ideal harmonic fields (thick dashed curves). There are some noticeable deviations, however, near the imaging- region boundaries (vertical dashed lines), which are caused either by discretization of the surface current or by not using large enough Q values in Eqs. [2], [3], [19], and [21] (to be discussed later). Typical design parameters for the aforementioned shim coils, including the condition number of the matrix D in Eq. [24] are listed in Table 1.

These results illustrate that the novel method presented here for designing shim coils allows decomposition of field harmonics into Fourier coefficients. To design a bi-planar shim coil with a finite radius, given any Fourier coefficient b_{nk}, the pure harmonic coil corresponding to the b_{nk} could be obtained easily and efficiently. We now address the following question: Since there are only harmonics associated with terms of $\cos k\phi$ in Eqs. [17] and (21), unlike Eq. [13], how can one design coils that generate harmonics associated with terms of $\sin k\phi$? To achieve this, we use T_{nk} and T'_{nk} to represent shim coils associated with terms of $\cos k\phi$ and $\sin k\phi$, respectively. Because $\sin k\phi = \cos\left[k\left(\phi - \frac{\pi}{2k}\right)\right]$, T'_{nk} shim coils can be designed directly by rotating T_{nk} shim coils by $90^\circ/k$. A T'_{21} shim coil that generates the harmonic $b_{21}r^2P_{21}(\cos\theta)\sin\phi$ can be obtained by a 90-degrees rotation of the T_{21} shim coils that generate $b_{21}r^2P_{21}(\cos\theta)\cos\phi$ field. In the same way, a T'_{31} shim coil can be obtained by rotating the T_{31} shim coil through 90 degrees; by rotating 45 degrees, T_{22} and T_{32} shim coils could be transformed into T'_{22} and T'_{32} shim coils, respectively; a 30-degrees rotation will transform a T_{33} shim coil into a T'_{33} coil. In other words, the other half of the tesseral harmonics coils, which are not covered by the aforementioned equations, can be obtained simply from rotating their counterparts.

DISCUSSION

Ill conditioning of the governing matrices is an unavoidable problem in most target-field methods for

Table 1 Parameters of the Shim Coils Designed Here, Including the Condition Number of the Matrix D in Eq. [24]

Coil Type	T_{20}	T_{21}	T_{22}	T_{32}	T_{33}
Optimal Q	5	3	4	3	5
Condition number	30	20	30	20	100
Shimming efficiency[a]	4.32 G/m^2/A	3.82 G/m^2/A	0.56 G/m^2/A	2.86 G/m^3/A	0.18 G/m^3/A
Computation time (s)	9.4	1.5	3.3	1.5	7.5

[a]Efficiencies are given in units of gauss.

coil design (*7*, *9*). Later we discuss how to scale well-conditioned and ill-conditioned systems of equations, how the conditioning of the governing matrices affects the design, and what are the advantages of our method in this regard.

Consider Eq. [24] as a governing matrix equation for the general target-field method. The vector A is formed from the coefficients that represent the target magnetic field; the vector U constitutes the unknown coefficients that determine the current distributions on the coil planes; and D is the matrix that describes the relationship between the field and source. The relationship between the relative change in the solution vector U to the change in the vector A is given by [see page 458 of (*16*)]:

$$\frac{\|\Delta U\|}{\|U+\Delta U\|} \le \|D\|\left\|D^{-1}\right\| \frac{\|\Delta A\|}{\|A\|}, \qquad [26]$$

where $\|D\|$ is the norm of the matrix D. One of the popular definitions of the norm is the uniform-matrix norm (*17*), which for an $m \times n$ matrix D is defined as

$$\|D\|_\infty = \max_{1<i<m} \sum_{j=1}^{n} \left|d_{ij}\right|. \qquad [27]$$

The relative error of vector A will be amplified by as much as $\mathrm{cond}(D) = \|D\|\left\|D^{-1}\right\|$, which is called the condition number of the matrix D. It is a scale for ill or well conditioning of the matrix equation. From this the maximum relative error of the solution can be described as $\mathrm{cond}(D)\times\varepsilon_{\mathrm{mach}}$, where $\varepsilon_{\mathrm{mach}}$ represents the machine epsilon, which on a 32-bit PC has the value $\varepsilon_{\mathrm{mach}} = 2^{1-32} = 5\times10^{-10}$. As a result, if the condition number of the governing matrix in a coil design is large compared to $1/\varepsilon_{\mathrm{mach}}$, the design result may not be trustworthy. The two ways to deal with this case are to use a higher-precision computer for the calculation or to solve the equation with other mathematical methods, such as Tikhonov regularization method (*9*, *10*).

One merit of the novel method presented here is that the condition number of the governing matrix is much smaller than other target-field methods. For instance, the condition numbers of matrices in designing a T_{20} shim coil with the same geometrical condition, using the new method and comparing to our previous work (*12*), are 30 (in Tables 1 and 2) and 1×10^{11}, respectively. The relative errors of the solutions on a 32-bit PC are 2×10^{-8} and 50, respectively. As a result, we can trust the design result of the novel method, but cannot rely on the second method unless reprocessing the calculation on a higher-precision computer or utilizing other mathematical methods. In fact our previous target-field method (*12*) is only suitable for designing gradient coils and not shim coils, which is why we developed this new approach.

We now discuss the design accuracy, coil efficiency, and computation time. With a larger Q, the coil can produce a shimming field more exactly equal to the ideal harmonic field. Nevertheless, the increase in Q also leads to more frequent mathematical oscillation of the computed surface current. The counteraction of the field caused by the frequently reversed current reduces the efficiency of the coils and

Table 2 Comparison of Condition Number and Relative Error for Some Typical Coils

	Novel Method			Previous Method (*12*)		
Coil type	T_{10}	T_{11}	T_{20}	T_{10}	T_{11}	T_{20}
Condition number	40	80	30	3×10^3	6×10^3	1×10^{11}
Relative error	2×10^{-8}	4×10^{-8}	2×10^{-8}	2×10^{-6}	3×10^{-6}	50

increases difficulty in their manufacture. Therefore, a compromise must be made between accuracy and efficiency. We found that when the series-expansion of the current is limited to $Q < 6$ terms, the approximate surface current obtained through matrix inversion meets the target field with reasonable accuracy. The coils designed here had little current oscillation and higher power efficiency with the optimal Q in Eqs. [2], [3], and [21]. In this work, neither Q (less than 6) nor N is large, which results in small-scale coefficient matrices and timesaving calculations. For example, when designing a T_{20} shim coil using the novel method with $Q = 5$ and cond $(D) = 30$, the computation time was 9.4 s on a PC with an Intel E8200 processor and 4 GB of memory. The computation times for the typical T_{nm} shim coils are listed in Table 1, along with their efficiencies. The coil efficiency is defined as b_{nm}/I_0, where b_{nm} is the harmonic coefficient of order n and degree m, and I_0 is the current flowing in the coil.

CONCLUSIONS

A novel analytical design methodology was developed by combining classical harmonic and popular target-field approaches. A matrix equation linking the field harmonics expressed by Fourier coefficients b_{nk} and the unknown surface current expressed by a Fourier series with weighting coefficients U_q has been established. The novel method describes the target field by giving the harmonic coefficients, instead of locating target-field points and specifying target-field values. Because this method does not require setting the target-field points, the governing matrix equation is better conditioned and more suitable for numerical solution.

Unlike with previous methods (*12*), it is feasible using this novel approach to design winding patterns for bi-planar shim coils. All bi-planar shim coils, including gradient coils for permanent-magnet MRI scanners, can be designed by the procedures established in this article. Each design result has been validated through the Biot-Savart law, i.e., by inserting the discrete current distribution obtained from the design procedure into the Biot-Savart formula to calculate the magnetic field that it generates. There is little deviation between the resulting field and the target field, which shows that the design method is effective and efficient. The new feature of this technique is that the specification of the target field is integrated more closely into the technique.

ACKNOWLEDGMENTS

This work is supported by the Natural Science Foundation of China (No.60871001). The authors thank Dr. H Guo and Dr. Y.V. Chang for reading the article earnestly and giving helpful discussions.

REFERENCES

1. Romeo F, Hoult DI. 1984. Magnet field profiling: analysis and correcting coil design. Magn Reson Med 1:44–65.
2. Morse PM, Feshbach H. 1953. Methods of theoretical physics. New York: McGraw-Hill.
3. Golay MJE. 1958. Field homogenizing coils for nuclear spin resonance instrumentation. Rev Sci Instrum 29:313–315.
4. Turner R. 1986. A target field approach to optimal coil design. J Phys D: Appl Phys 8:L147–L151.
5. Turner R. 1994. Electrical Coils. United States: British Technology Group Limited (London, GB2), assignee.
6. Jin J-M. 1999. Electromagnetic Analysis and Design in Magnetic Resonance Imaging. Boca Raton: CRC Press.
7. Brideson MA, Forbes LK, Crozier S. 2004. Winding patterns for bi-planar MRI shim coils with rectangular and circular target-field regions. Meas Sci Technol 15:1019–1025.
8. Liu H, Truwit CL. 1998. True energy-minimal and finite-size bi-planar gradient coil design for MRI. IEEE Trans Med Imag 17:826–830
9. Forbes LK, Crozier S. 2004. Novel target-field method for designing shielded bi-planar and gradient coils. IEEE Trans Magn 40:1929–1938.
10. Forbes LK, Brideson MA, Crozier S. 2005. A target-field method to design circular bi-planar coils for asymmetric shim and gradient fields. IEEE Trans Magn 41:2134–2144.
11. Ungersma SE, Xu H, Chronik BA, Scott GC, Macovski A, Conolly SM. 2004. Shim design using a linear programming algorithm. Magn Reson Med 52:619–627.
12. Liu W, Zu D, Tang X, Guo H. 2007. Target-field method for MRI bi-planar gradient coil design. J Phys D: Appl Phys 15:4418–4424.
13. Griffiths DJ. 1998. Introduction to Electrodynamics, 3rd ed. Prentice Hall, New Jersey. pp. 219.
14. Abramowitz M, Stegun IA. 1972. Handbook of Mathematical Functions. New York: Dover.
15. Tomasi D. 2001. Stream function optimization for gradient coil design. Magn Reson Med 45:505–512.
16. Atkinson KE. 1978. An introduction to Numerical Analysis. New York: Wiley. p 458.
17. Golub G, Van Loan CF. 1996. Matrix Computations, 3rd ed. Baltimore: The Johns Hopkins University Press. pp 56–57.